IET Research Journals

Continuous Frequency and Bandwidth Tunable Combline Cavity Bandpass Filters with Internally Mounted Motors

ISSN 1751-8644
doi: 0000000000
www.ietdl.org

J.S. Parish[1] *N. Somjit*[1] *I.C. Hunter*[1]

[1] Pollard Institute, School of Electronic and Electrical Engineering, University of Leeds, LS2 9JT, UK
** E-mail: ml07j2p@leeds.ac.uk*

Abstract: Novel design methods for implementing continuous centre-frequency and bandwidth tunability are reported. Coupling bandwidths are tuned through the mechanical rotation of a metallic plate suspended between resonators. Centre-frequency tuning is achieved via the vertical actuation of a moving part mounted within each resonator. In addition, each resonator and transformer is designed so that motors can be housed within them — adding tunability without compromising the overall filter volume. A second-order filter, based on Combline cavity structures, capable of bandwidth tunability of $49\,\mathrm{MHz}$ to $67\,\mathrm{MHz}$ for all centre-frequencies in the range of $1.751\,\mathrm{GHz}$ to $1.998\,\mathrm{GHz}$ is presented. Passband insertion loss is kept below $1.2\ \mathrm{dB}$ for all tuning states with return loss above $10\ \mathrm{dB}$. A five-pole filter is also fabricated with centre-frequency tunability of 14% from $1.764\,\mathrm{GHz}$ to $2.015\,\mathrm{GHz}$ and $15\ \mathrm{dB}$ bandwidth tunability of 107% from $41\,\mathrm{MHz}$ to $85\,\mathrm{MHz}$. Midband insertion loss is kept below $1.4\ \mathrm{dB}$ in all tuning states. The five-pole filter is compared to other tunable filters in the UHF range and is shown to reduce midband insertion loss by 36% from the next best filter ($2.2\,\mathrm{dB}$ to $1.4\,\mathrm{dB}$).

1 Background

Demand for tunable filtering in the cellular telecommunications industry has always been high. Particularly in cellular base stations where on-the-fly adaptability of a single piece of hardware can fulfil the role of multiple components - reducing the total space, weight and cost associated with said components.

Tunable filter designs pose many challenges. Early tuning methods utilised YIG spheres as a means to provide resonance tuning as a function of an externally applied DC magnetic field [1]. Despite having wide tuning ranges and high Q-factors they suffered from being too bulky to keep up with the demand for miniaturisation as well as effects of hysteresis and high power consumption.

Varactor diodes provide capacitive tuning by exploiting a change in the depletion layer width as a function of applied DC bias. In filtering applications varactor diodes have been extensively explored however they typically exhibit low Q-factors [2] and due to poor intermodulation performance struggle to handle power signals larger than $1\ \mathrm{mW}$ [3].

Barium Strontium Titanate (BST) varactors allow for the capacitance to be altered by exploiting the ferroelectric phases in order to control the dielectric constant of a material with a voltage bias. As with varactor diodes Q-factor and linearity are again the limiting factors [4–9].

PIN diodes act as RF switches and can be used in filters for switching between multiple passband states. Again, Intermodulation distortion and resistive losses inhibit their effectiveness in high performance filtering applications [10–12].

In more recent times MEMS devices have pushed the state of the art with very low power consumption, high isolation, low insertion loss and good suppression of intermodulation products. However due to their size, drawbacks include power handling, mass production costs and reliability [13–16].

Mechanically tuned filters can overcome issues of intermodulation distortion generated by discrete components[17–19], however they require the mounting of motors in order to provide the required actuation, which can significantly increase the volume of the filter.

In this paper, prototype filters with a centre-frequency of $2\ \mathrm{GHz}$ and bandwidth of $40\ \mathrm{MHz}$ with 14% frequency tunability from $1.75\ \mathrm{GHz}$ to $2\ \mathrm{GHz}$ and bandwidth tunability of 50% from $40\ \mathrm{MHz}$ to $60\ \mathrm{MHz}$ are fabricated. Commercially available stepper motors are shown to fit comfortably within the filter confirming that tunability can be achieved without having to sacrifice overall filter volume.

The fabricated filters introduce three novelties in the design of a fully tunable filter with precise bandwidth and centre-frequency control. A novel method for the implementation of inter-resonator coupling tunability is described. Secondly, a new technique which provides tuning for both resonant frequency and external coupling is presented. Lastly, resonators and transformers are designed in such a way that the motors can be contained inside them. This allows for the cavitys external dimensions to remain unchanged despite the added complexity of tunability being provided.

2 Design

2.1 Bandwidth tunability

In a combline filter the inter-resonator coupling is represented as a short-circuited transmission line where its admittance between the rth and $(r+1)$th resonators can be calculated for a given electrical length (θ_0) as follows [20]:

$$Y_{r,r+1} = \frac{K_{r,r+1}\tan(\theta_0)}{n_r n_{r+1}} \tag{1}$$

Where $K_{r,r+1}$ are given by the inverter coupled low pass prototype. n_r can be calculated using the shunt capacitances of the prototype, C_{Lr}.

$$n_r = \sqrt{\frac{\alpha C_{Lr}\tan(\theta_0)}{Y_{rr}}} \tag{2}$$

α is the bandwidth scaling factor, and Y_{rr} can be equated to 1 for simplicity.

The addition of a tunable capacitor in parallel to the coupling provides a means for adjusting tunability. Suspension of a single plate between two resonators provides a capacitance in parallel with the coupling. Rotation of the plate through its vertical centre line

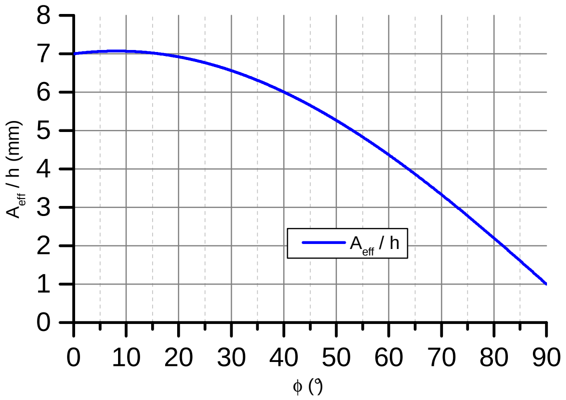

Fig. 1: Change in the normalised effective plate area A_{eff}/h, of a rotating plate as seen by the resonators

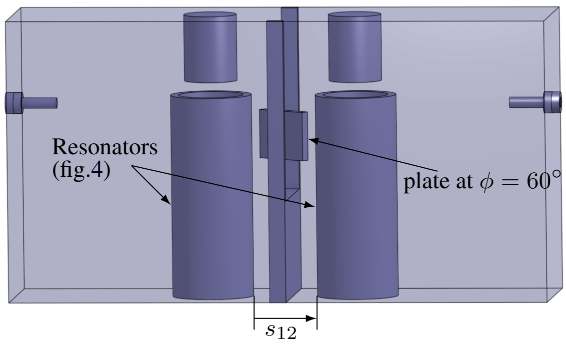

Fig. 2: Side-view of a three-dimensional structure of two cylindrical resonators coupled via a rotating plate in an iris

changes the effective plate area as seen by the resonators and subsequently changes the overall coupling. Control of the coupling can therefore be achieved via the rotational position of the plate.

Fringing capacitance, C_f is non-zero and affects the overall capacitance between resonator and plate additively such that:

$$C = C_p + C_f \tag{3}$$

The effective plate area A_{eff}, seen by the resonators can be calculated as a function of the plate width w (mm), height h (mm), thickness t (mm), and angle of rotation ϕ ($^\circ$) as follows

$$A_{eff}(\phi) = h[w \sin(90 - \phi) + t \cos(90 - \phi)] \tag{4}$$

Which can be normalised per plate height and simplified to

$$\frac{A_{eff}(\phi)}{h} = w \cos(\phi) + t \sin(\phi) \tag{5}$$

Figure 1 shows how A_{eff}/h changes with ϕ for a plate of width 7 mm and thickness 1 mm. Scrutiny of the graph shows how the effective plate area changes in a linear-like fashion from $\phi = 30^\circ$ to 90° for this ratio of width to thickness.

It follows that due to the proportionality of plate area to capacitance, it can be expected that the capacitance between a rotating plate and a resonator would change in a linear-like fashion across the same range of ϕ, where $C_p \gg C_f$.

Eigenmode simulation was employed in order to determine the range of coupling bandwidths achievable as the plate is rotated through 90°, ie maximum to minimum plate area as seen by the resonators.

The simulation of the three-dimensional structure was set up as in figure 2 with two coaxial-resonators (figure 4) contained within an enclosed cavity and coupled via a fixed iris. A single plate with a thickness of $t = 1$mm and width $w = 7$mm, was suspended in the centre of the iris, equidistant from each resonator.

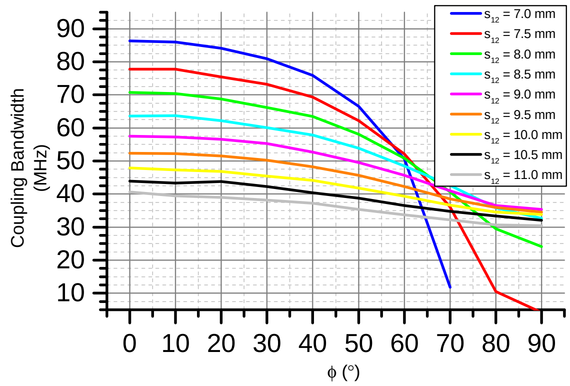

Fig. 3: Simulation of coupling bandwidths against ϕ for given resonator spacings (s_{12})

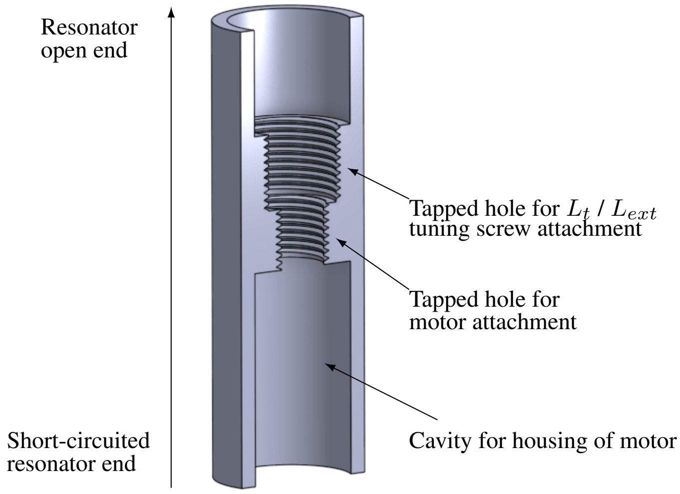

Fig. 4: Physical design shape of resonators (and transformers) with the front section removed

Figure 3 shows a graph plotting the range of coupling bandwidths observed when rotating the plate from 0° to 90° for given resonator spacings ($s_{12} = 7$ mm to 11 mm). The plate is deemed to be at an angle of 0° when the flat edges of the plate face the resonators, and 90° when facing the ground-plane side walls of the cavity.

For resonator spacings of a similar size to w, the couplings become very sensitive as ϕ approaches 90°. This is because the sides of the plate come into close proximity to the resonators at these angles. Consequently C_p becomes very large and so the coupling bandwidths rapidly tend towards zero. For a realised filter this would be impractical since its response would become sensitive to ambient vibrations and other environmental disturbances in the vicinity of the filter.

Conversely, for resonator spacings of $s_{12} \geq 9.5$ mm, the distance between resonator and plate is large enough that the capacitive effects of plate rotation have diminishing impact on the coupling bandwidth as s_{12} increases.

Therefore careful consideration of resonator spacing must be taken in order to determine the optimum coupling tunability for the specification without the system becoming sensitive to external influence.

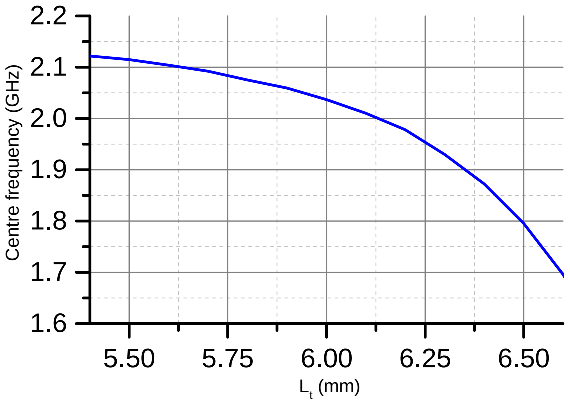

Fig. 5: Simulated centre-frequency tuning of a second order filter with inner-screw actuation

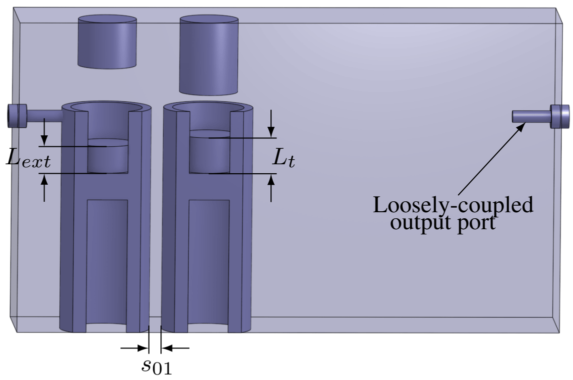

Fig. 6: Simulation setup for calculation of external couplings. Front sections have been removed from the transformer and first resonator to expose the L_{ext} and L_t tuning screws.

2.2 *Resonant frequency and external coupling tunability*

Combline resonators are short-circuited lines that are capacitively loaded to ground on the open end. In coaxial cavity resonators this capacitance is usually realised by an air gap between the resonator end and cavity lid. Traditional methods for tuning resonant frequency utilise discrete components mounted outside the cavity to tune the capacitance to ground. Low Q due to inherent component losses as well as low power handling capabilities are drawbacks to this type of tunability. Other methods use mechanical actuation of tuning screws or disks grounded via the cavity lid to tune resonance. Metal-air-metal capacitive loading allows for a much higher Q to be retained than when fixed components are used. Here a new method for mechanical tuning is presented.

Treating the resonator as a hollow cylinder allows for a vertical linear actuating screw to be attached within. Actuation of the screw in a vertical direction simultaneously modifies the resonator's physical length as well as its capacitance to ground. Both of these effects combine to tune the frequency of resonance synchronously. This also provides the added benefit of being able to mount a motor within the hollow resonator in the unused space beneath the screw it actuates. Thus a filter with resonant frequency tuning capabilities can be realised without the need to increase the filters overall volume.

Incidentally, the same actuation technique can be performed on a dielectric material — tuning the effective absolute permittivity between the resonator end and ground. Proximity to ground would then no longer be an issue. Remembering capacitance is proportional to permittivity. Therefore the tuning range can be increased or decreased by selecting a material with an appropriate dielectric constant for the desired tunability. Dielectric means of resonance tuning come at the expense of resonator quality factor however due to the introduction of dielectric losses to the resonator.

The graph in figure 5 shows the centre-frequency tuning range of a simulated two-pole filter. In a narrowband coaxial resonator filter, external coupling is provided by impedance transforming elements. When realised these transformers are TEM lines that resonate well above the passband. Because of this property, tuning for external coupling can be provided using the same methods as resonant tuning.

External couplings Q_e can be calculated by looking at the reflected group delay T_d, of an EM simulation where only the input transformer and first resonator are modelled in the cavity - shown in figure 6. The output port is then loosely coupled so as to not affect the results. External coupling is given by

$$Q_e = \frac{\omega_0 T_d}{4} \tag{6}$$

Calculated Q_e for tuning screw actuation L_{ext}, at given input spacings s_{01}, are shown in figure 7. It is clear that at first glance, the tuning range of Q_e is much smaller than for the inter-resonator coupling bandwidths of figure 3. Therefore the limiting factor in terms of the overall tunability of a fully tunable filter is the external coupling.

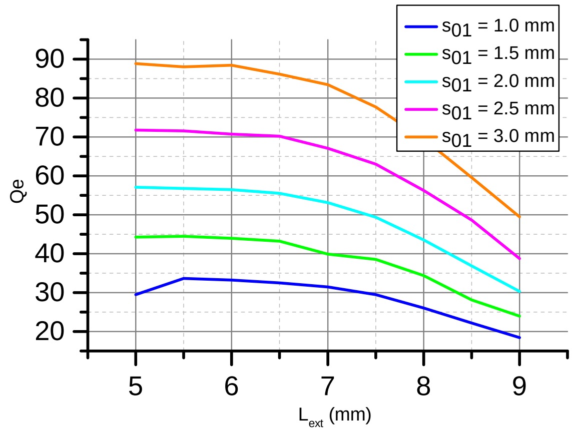

Fig. 7: Q_e tuning for different input spacings, s_{01}

Once the tuning ranges for each of the couplings have been calculated, the N+2 coupling matrix [21] can be used in order to determine the tuning limits of a fully tunable filter implementing the tested tuning structures.

3 Implementation

3.1 *Prototype design*

The simultaneous utilisation of tuning mechanisms for resonance, inter-resonator coupling and external coupling, presented in the previous section, allows the design of a fully tunable filter with control over centre-frequency, bandwidth and return loss.

An increase in loading capacitance on the TEM lines lowers the resonant frequency, design of the filter can be made to the specification of the highest frequency passband desired - in this case, 2 GHz. This means that the resonant tuning mechanism L_t, is in its lowest position — where it has little effect on the resonance. Increasing L_t causes a reduction in the centre-frequency. Similarly for the external coupling the ripple level lowers as the centre-frequency is reduced. Recovery of the ripple level is made by reducing the external coupling. Therefore the design of the filter can be made on the assumption that tuning mechanisms L_t and L_{ext} are small enough not to be significantly affecting the response - allowing the maximum tuning range available.

In addition to designing the filter at its highest frequency specification, it is also be designed at its narrowest bandwidth. As the bandwidth is increased the ripple level lowers. As before, the external coupling can be tuned in order to restore the return loss to the desired level.

Table 1 Comparison of Tunable Microwave Filters in the UHF range

Source	Tuning Method	Centre-Frequency (GHz)	Bandwidth (MHz)	Passband Return Loss (dB)	Passband Insertion Loss (dB)
[17]	Mechanical	1.98-2.03	20-25	-	-
[18]	Mechanical	-	11-33	-	-
[19]	Mechanical	2.565-2.635	-	> 16.2	< 2.3
[19]	MEMS	2.59-2.634	-	> 15	< 4.25
[24]	Varactor	0.55-1.1	34-66	> 10	-
[25]	Varactor	2.4-2.6	-	> 10	< 3.4
[26]	Varactor	1.66-2.4	-	> 10	< 3
[27]	MEMS	1.5-2.5	105-125	> 10	< 2.2
[28]	MEMS	0.6-1.1	-	-	< 3.6
this work	Mechanical	1.764-2.015	41-85	> 11.3	< 1.4

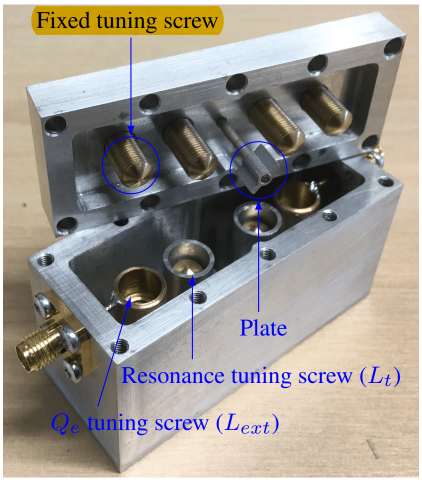

Fig. 8: Photograph showing the fabricated fully tunable second order prototype filter

Realisation of the plate providing inter-resonator coupling is a key component in the operation of the filter. It must not be electrically connected to ground as this would hinder its performance significantly. In addition it must be positioned at the correct height - near level with the top of the resonators. This is where the electric field is at its strongest hence allowing for optimum capacitive tunability. The plate is suspended on the end of a screw fabricated in polyether ether ketone (PEEK) - a polymer chosen for its high tensile strength and large loss tangent [22].

The filter cavity and resonators are cut from a single block of aluminium. A thread is tapped on the inside of the hollow resonators, so that the L_t tuning screws can be attached inside. A similar procedure was also performed on the transformers for the L_{ext} tuning screws. The small input spacing (s_{01}) means that milling the transformers from the original aluminium block is impossible. Therefore the transformers are required to be fabricated separately in brass and plated in copper before being mechanically pressed into the filter cavity. Copper plating of the transformers is required only for the ease of soldering input connectors.

After fabrication, fixed tuning screws are mounted from the lid above each resonator and transformer (see figure 8) in order to correct for tolerances in the fabrication processes. These are used to set the filter to a fundamental specification of centre frequency and bandwidth (2GHz and 60 MHz respectively) before being locked in place by fixing nuts on the outside of the cavity. It is important to emphasize that these screws, once fixed are never again altered. All subsequent tunability of the filter is provided by the novel mechanisms introduced by this paper and illustrated in figures 2 and 6.

The prototype filter is designed to be tunable from 1.75 GHz to 2 GHz with 10 dB bandwidths from 40 MHz to 60 MHz at both frequencies. Figure 9 shows a comparison of simulated to measured results. At a centre-frequency of 1.751 GHz a bandwidth tuning range of 49 MHz to 70 MHz is observed. Similarly at 1.998 GHz

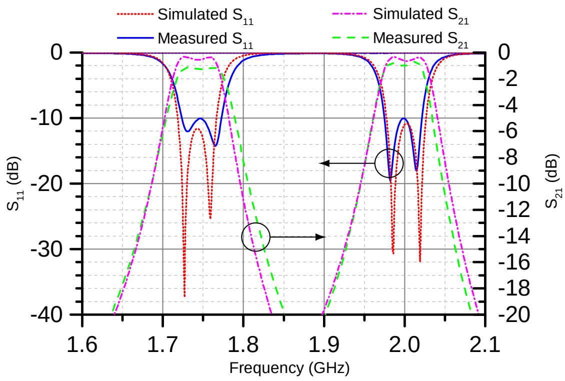

(a) Narrow bandwidth responses

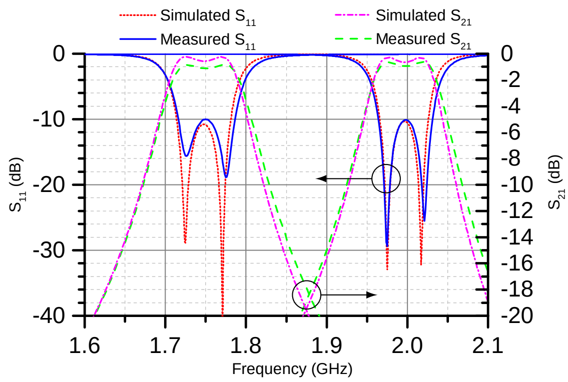

(b) Wide bandwidth responses

Fig. 9: A comparison of simulated to measured responses for a fully tunable two-pole prototype filter at centre-frequencies of 1.75 GHz and 2 GHz overlayed on the same axes for (a) Narrow-bandwidth tuned states, (b) wide-bandwidth tuned states.

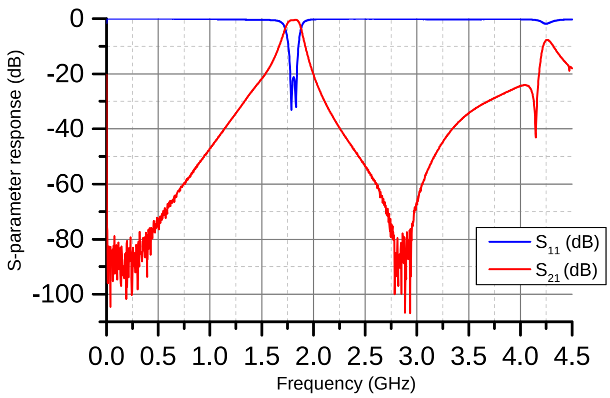

Fig. 10: Broadband S-parameter measurements of two-pole prototype showing the spurious-free window

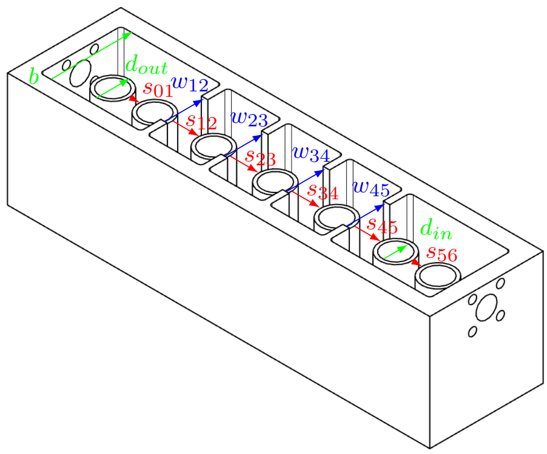

Fig. 11: Configuration of fifth order design

bandwidth tunability from 41 MHz to 67 MHz is achieved. Across the entire tuning range, passband insertion loss is less than 1.2 dB. Good correlation between simulation and measured responses can be seen showing that the prototype performs as intended. Figure 10 shows a broadband response for the filter at a centre frequency of 1.8 GHz. Two transmission zeros are seen above the passband. The first is introduced due to dispersive coupling where the electric coupling introduced by the plate cancels with the dominant inductive coupling of a typical combline [23]. The second transmission zero is typical for a combline filter and occurs at the quarter-wave frequency of the TEM lines [20]. The first spurious band is located at 4.2 GHz and is partially suppressed by a transmission zero introduced as an effect of the capacitive coupling mechanism.

3.2 *Fifth order fully-tunable filter*

A fifth order version of the filter measured in the previous section was designed and fabricated in aluminium using the same tunability specifications as before (figure 13). The dimensions of the filter were estimated through combline design processes outlined in [20] and optimised for 15 dB bandwidths using HFSS. Table 2 shows the optimised dimensions of the filter. Tuning of the inter-resonator couplings is provided via manual rotation of the PEEK screws attached to the plates. Additional work could introduce rotary motors to mechanically couple to the PEEK screws and drive the actuation. This, in conjunction with the resonator and transformer motors would allow for the filter to be fully controllable from a remote location.

Observation of the measured results (figure 12) shows the filter's tunability in both frequency and bandwidth. The centre-frequency is shown to be tunable from 1.764 GHz to 2.015 GHz with bandwidth ranges of 61 MHz to 85 MHz and 41 MHz to 69 MHz at each respective centre-frequency.

Passband insertion loss was typically seen to be about 1 dB and the worst midband insertion loss was measured at 1.4 dB. The achieved unloaded Q for the filter cavities was calculated for each of the four tuned states from figure 12. These are shown in table 3. As would be expected, the unloaded Q is seen to decrease with frequency tuning. Increasing the size of the cavity would increase the achievable Q at the expense of overall volume.

Drawbacks to this design lie in the mechanical aspects. For example, tuning elements L_t and L_{ext} have limited contact with the resonators and transformers respectively. The contact is limited by the threads of the screw, since in reality the screw-threads do not perfectly overlap. This contact becomes worse the more the screws are actuated because there are fewer threads connecting the screw to the resonator. Self-locking screws would help to overcome this issue to some extent by ensuring a good contact is made at all times.

Table 1 shows a comparison of tunable filter designs from other papers to the work presented here. The filter presented in this work

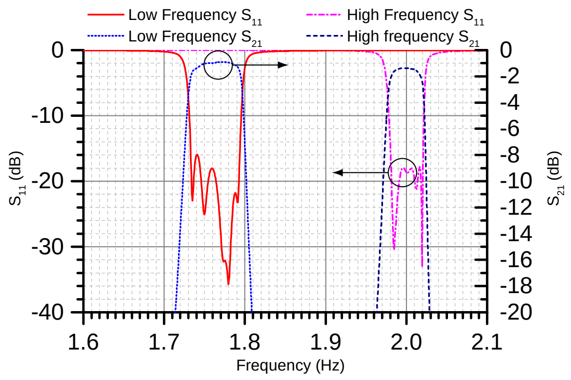

(a) Narrow bandwidth responses

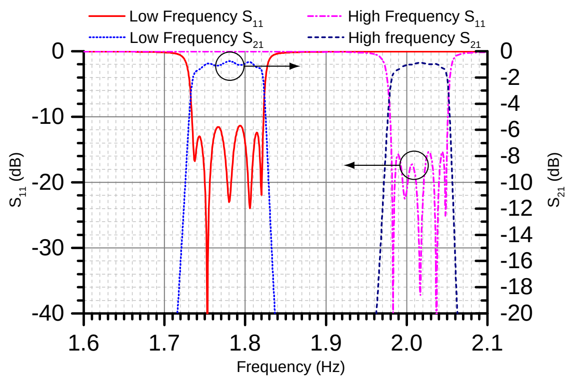

(b) Wide bandwidth responses

Fig. 12: Measured S-parameter responses for the fifth order filter with centre-frequency and bandwidth control

Table 2 Dimensions of the 5-pole filter from figure 11

Parameter name	Symbol	Value (mm)
Resonator spacing (0-1)	$s_{01}\ (= s_{56})$	3
Resonator spacing (1-2)	$s_{12}\ (= s_{45})$	8.2
Resonator spacing (2-3)	$s_{23}\ (= s_{34})$	9
Iris width (1-2)	w_{12}	12.8
Iris width (2-3)	$w_{23}\ (= w_{34})$	12
Iris width (4-5)	w_{45}	12.4
Plate width	w	7
Plate height	h	6
Plate thickness	t	1
Resonator outer diameter	d_{out}	10
Resonator inner diameter	d_{in}	8
Ground plane spacing	b	25

Table 3 Acheived unloaded Q of filter cavities for each tuned state from figure 12.

Bandwidth	Low frequency state	High frequency state
Narrow	900	1000
Wide	900	1050

shows a good level of frequency and bandwidth tunability while maintaining low insertion loss in comparison to other works.

4 Conclusion

This paper presents novel methods for the tuning of inter-resonator couplings, external couplings and resonant frequency. In addition, resonators are designed with cavities to house actuation motors

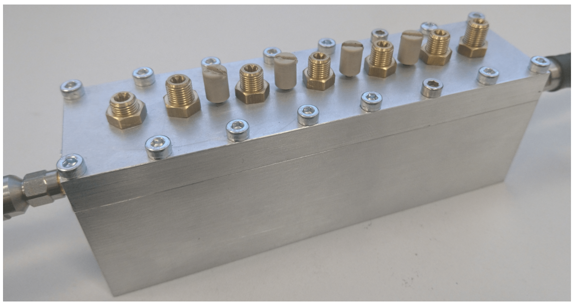

(a) Photograph showing the fabricated fully tunable 5-pole filter

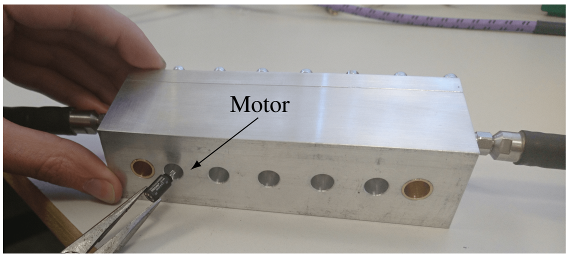

(b) Photograph of a commercially available stepper motor being inserted into a resonator cavity

(c) Motor shown inside resonator cavity

Fig. 13: Fabricated five-pole filter with internal mounting of motor

within — adding tunability to the filter without compromising volume. Two filters were designed, fabricated and measured. Firstly, a two-pole filter was shown to be able to tune centre-frequency from 1.751 GHz to 1.998 GHz with continuous bandwidth control from 49 MHz to 67 MHz achievable throughout the range. Passband insertion loss was kept under 1.2 dB in all states.

A five-pole filter was also fabricated to the same filtering specifications. Centre-frequency tunability was shown from 1.764 GHz to 2.015 GHz with bandwidths from 40 MHz to 85 MHz. The maximum midband insertion loss was shown to be 1.4 dB.

The overall tunability of this design is limited by the tuning range of the external coupling. A different method that allows for a larger range of external Q tuning could lead to a better all-round tuning performance. There is an inherent trade-off between tuning range and sensitivity with this design. A higher tuning range would be achievable by reducing the filter spacings, however any mechanical vibrations might then have an effect on the filter response.

This work could be extended by replacing the metallic actuating screws with dielectric materials. Frequency tunability would be increased relative to the dielectric constant of the material used at the expense of filter Q. In addition, provision of independent motors controlling the individual resonances and couplings, the resolution of tunability can be estimated by collating data from figures 3, 5 and 7 for inter-resonator coupling, resonance and external coupling respectively with achievable step angles of motors and the thread pitch of screws used. Empirical testing would then allow for a lookup table to be generated for the absolute positions of each tuning mechanism for the desired filtering response.

Acknowledgement

The author would like to acknowledge Radio Design Ltd. for their on going support and advice, as well as providing access to their facilities for this work.

5 References

1 J. D. Adam, L. E. Davis, G. F. Dionne, E. F. Schloemann, and S. N. Stitzer, "Ferrite devices and materials," *IEEE Transactions on Microwave Theory and Techniques*, vol. 50, no. 3, pp. 721–737, Mar 2002.

2 A. R. Brown and G. M. Rebeiz, "A varactor-tuned rf filter," *IEEE Transactions on Microwave Theory and Techniques*, vol. 48, no. 7, pp. 1157–1160, Jul 2000.

3 S. R. Chandler, I. C. Hunter, and J. G. Gardiner, "Active varactor tunable bandpass filter," *IEEE Microwave and Guided Wave Letters*, vol. 3, no. 3, pp. 70–71, March 1993.

4 A. Tombak, J. P. Maria, F. T. Ayguavives, Z. Jin, G. T. Stauf, A. I. Kingon, and A. Mortazawi, "Voltage-controlled rf filters employing thin-film barium-strontium-titanate tunable capacitors," *IEEE Transactions on Microwave Theory and Techniques*, vol. 51, no. 2, pp. 462–467, Feb 2003.

5 A. Vorobiev, P. Rundqvist, K. Khamchane, and S. Gevorgian, "Silicon substrate integrated high q-factor parallel-plate ferroelectric varactors for microwave/millimeterwave applications," *Applied Physics Letters*, vol. 83, no. 15, pp. 3144–3146, 2003.

6 X. Wang, P. Bao, T. Jackson, and M. Lancaster, "Tunable microwave filters based on discrete ferroelectric and semiconductor varactors," *Microwaves, Antennas Propagation, IET*, vol. 5, no. 7, pp. 776–782, May 2011.

7 V. Pleskachev and I. Vendik, "Tunable microwave filters based on ferroelectric capacitors," in *Microwave and Telecommunication Technology, 2003. CriMiCo 2003. 13th International Crimean Conference*, Sept 2003, pp. 468–470.

8 C. Y. Tan and C. K. Ong, "Planar tunable HTS microwave filter with patterned ferroelectric thin film," *Superconductor Science and Technology*, vol. 19, no. 2, p. 212, 2006. [Online]. Available: http://stacks.iop.org/0953-2048/19/i=2/a=010

9 J. Nath, D. Ghosh, J.-P. Maria, A. I. Kingon, W. Fathelbab, P. Franzon, and M. Steer, "An electronically tunable microstrip bandpass filter using thin-film Barium-Strontium-Titanate (BST) varactors," *Microwave Theory and Techniques, IEEE Transactions on*, vol. 53, no. 9, pp. 2707–2712, Sept 2005.

10 H. Shurner, *Microwave Semiconductor Devices*. Pitman and sons, 1971.

11 Z. Brito-Brito, I. Llamas-Garro, G. Navarro-Muñoz, J. Perruisseau-Carrier, L. Pradell, F. Giacomozzi, and S. Colpo, "Precise frequency and bandwidth control of switchable microstrip bandpass filters using diode and microelectro-mechanical system technologies," *Microwaves, Antennas Propagation, IET*, vol. 6, no. 6, pp. 713–719, April 2012.

12 C. Lugo and J. Papapolymerou, "Electronic switchable bandpass filter using pin diodes for wireless low cost system-on-a-package applications," *IEE Proceedings - Microwaves, Antennas and Propagation*, vol. 151, no. 6, pp. 497–502, Dec 2004.

13 A. Abbaspour-Tamijani, L. Dussopt, and G. Rebeiz, "Miniature and tunable filters using MEMS capacitors," *Microwave Theory and Techniques, IEEE Transactions on*, vol. 51, no. 7, pp. 1878–1885, July 2003.

14 D. Girbau, N. Otegi, L. Pradell, and A. Lazaro, "Study of intermodulation in RF MEMS variable capacitors," *Microwave Theory and Techniques, IEEE Transactions on*, vol. 54, no. 3, pp. 1120–1130, March 2006.

15 G. Rebeiz and J. B. Muldavin, "RF MEMS switches and switch circuits," *Microwave Magazine, IEEE*, vol. 2, no. 4, pp. 59–71, Dec 2001.

16 C. yuan Lee and E. S. Kim, "Piezoelectrically actuated tunable capacitor," *Microelectromechanical Systems, Journal of*, vol. 15, no. 4, pp. 745–755, Aug 2006.

17 M. Yuceer, "A reconfigurable microwave combline filter," *IEEE Transactions on Circuits and Systems II: Express Briefs*, vol. 63, no. 1, pp. 84–88, Jan 2016.

18 A. I. Abunjaileh and I. C. Hunter, "Combline filter with tunable bandwidth and centre frequency," in *2010 IEEE MTT-S International Microwave Symposium*, May 2010, pp. 1476–1479.

19 S. Fouladi, F. Huang, W. D. Yan, and R. R. Mansour, "High-*q* narrowband tunable combline bandpass filters using mems capacitor banks and piezomotors," *IEEE Transactions on Microwave Theory and Techniques*, vol. 61, no. 1, pp. 393–402, Jan 2013.

20 I. C. Hunter, *Theory and Design of Microwave Filters*. The Institution of Engineering and Technology, 2001.

21 R. Cameron, C. Kudsia, and R. Mansour, *Microwave Filters for Communications Systems: Fundamentals, Design, and Applications*. John Wiley and sons, 2007.

22 "Victrex materials properties guide," http://www.victrex.com/~/media/literature/en/material-properties-guide_us-4-20.pdf, Online: accessed November 2017.

23 A. Anand and X. Liu, "Substrate-integrated coaxial-cavity filter with tunable center frequency and reconfigurable bandwidth," *WAMICON 2014, Tampa, FL*, pp. 1–4, 2014.

24 A. Anand and X. Liu, "Reconfigurable planar capacitive coupling in substrate-integrated coaxial-cavity filters," *IEEE Transactions on Microwave Theory and Techniques*, vol. 64, no. 8, pp. 2548–2560, Aug 2016.

25 S. Sirci, J. D. Martinez, R. Stefanini, P. Blondy, and V. E. Boria, "Compact smd packaged tunable filter based on substrate integrated coaxial resonators," in *2014 IEEE MTT-S International Microwave Symposium (IMS2014)*, June 2014, pp. 1–4.

26 Y. Liang and S. Kumar, "Electronically tunable microstrip combline filter," *Canadian Journal of Electrical and Computer Engineering*, vol. 15, no. 3, pp. 123–128, Aug 1990.
27 M. A. El-Tanani and G. M. Rebeiz, "High-performance 1.5-2.5 ghz rf-mems tunable filters for wireless applications," *IEEE Transactions on Microwave Theory and Techniques*, vol. 58, no. 6, pp. 1629–1637, June 2010.
28 Y. Shim, Z. Wu, and M. Rais-Zadeh, "A high-performance continuously tunable mems bandpass filter at 1 ghz," *IEEE Transactions on Microwave Theory and Techniques*, vol. 60, no. 8, pp. 2439–2447, Aug 2012.